27 May 1955

HIGH ALTITUDE OBSERVATORY
of the
University of Colorado

Solar Research Memorandum No. 37

From: D. E. Billings and Carlos Varsavsky

Subject: An Absolute Calibration of the Climax Intensity Scale for Coronal Lines.*

INTRODUCTION

Until very recently almost every coronal observatory has reported emission line intensities in a different scale. Arosa, Kanzelhohe and Wendelstein have used a 50-step "memory scale", that could, if needed, be expanded. Climax and Sacramento Peak have recorded their spectra photographically and have visually compared the densities of the lines on the photographic plates with those on a comparison "wedge", the resulting scale covering the range 0-40. Only Pic du Midi and Mt. Norikura reported line intensities in terms of the intensity of one angstrom of the light from the solar disk at the same wavelength as the line (equivalent angstroms).

Because of the extremely stringent requirements on observing conditions for obtaining good quality coronal measures, each coronagraph station experiences quite a number of days in which no trustworthy observations are made. Analysts have attempted to combine observations from various stations so as to obtain as nearly complete a set of line intensities as possible. Several of these analysts, notably Behr (1951), Bell and Glazer (1953) and Bruzek (1955) have carried out statistical comparisons of the intensities as measured by various stations in order to establish tables for conversion of the readings of one station into the scale of the other.

In the meantime Commission 11 of the International Astronomical Union (Trans. I. A. U., 1952) recommended that all stations express coronal intensities in terms that can be intercompared, in view of the wide discrepancies. Waldmeier (1951) and Kraul (1954) have described methods used for standardizing the visual memory scales at Arosa and Wendelstein, respectively.

Although Climax coronal line intensities have been reported in an arbitrary scale prior to January, 1955, Dr. Walter Orr Roberts early

---

*The work reported in this memorandum has been supported by the Office of Ordnance Research under Contract No. DA-23-072-ORD-764.

recognized the need of taking data in such a way as to insure that the scale would have a uniform meaning in terms of line intensities, and in 1944 began the practice of using a sensitometer to place a set of eight photometric spots on every spectrograph plate. In the sensitometer the light forming the spots passed through a green filter with a transmission band centered near 5303 Å, then through various geometrical apertures to impress graded intensities on the film to produce the spots. The lamp was connected to a power supply with a carefully controlled voltage considerably below its rated voltage so as to minimize aging of the filament and bulb. In the routine operation used prior to 1955, the plates, after removal from the spectrograph, have been exposed in the sensitometer for the same length of time as used in taking the spectra, then have been developed in such a way as to effect the same spot densities, within certain limits, for all plates. After the plates were developed, a "wedge" containing approximately fifteen comparison lines, with profiles resembling those of coronal lines and various degrees of density, was placed on the plate beside the coronal line, and the comparison line was found that best corresponded to the coronal line.

The procedure has certain definite advantages over the memory scales used at Wendelstein and Arosa: The comparison lines are available as a reference at all times; they are viewed against the same background of density due to scattered light as the coronal lines; and the numbers in the 0-40 scale assigned to them are such that the resulting arbitrary intensities are approximately linear (in the case of a typical photographic characteristic curve) in their relation with the actual intensities of the lines.

There are several difficulties inherent to the method, however, the foremost being that no equivalence was established between the units on the arbitrary scale and any absolute scale. Another difficulty is that although the photographic characteristic curves for the various plates may be kept the same (within limits) for the green light used in forming the spots, changes in emulsion bring about uncontrollable changes in the characteristics at the wavelengths of the red and yellow coronal lines. Occasionally, also, the observers do not succeed in controlling the photography within the prescribed limits. As a result, quite a number of plates each year have been ruled as yielding low weight data, even though perfectly good photographs of coronal spectra were present on them. Finally, since, in the reading of the plates, the superposition of the comparison wedge on the spectrum of the scattered light adds densities of the wedge and plate, whereas, in taking the photograph, the intensities of the coronal line and scattered light are added, adequate correction for various scattered light intensities is not provided.

The High Altitude Observatory staff, working under the auspices of the U. S. Office of Ordnance Research, has recently completed a program

with the dual purpose of developing a set of tables suitable for conversion of Climax line intensities already reported from the arbitrary scale into equivalent Angstroms and setting up routine procedures whereby all Climax data reported in the future will be in absolute units. Through this program we have attempted to correct for the difficulties in the earlier procedures, so that absolute intensities obtained from the older readings and intensities to be reported in the future will essentially be independent of the brightness of scattered light and the emulsion characteristics.

PROCEDURE

A. General Outline.

In brief outline, the steps of the standardization procedure which we used were as follows: (1) We made microphotometer tracings of coronal lines on many plates from the library of Climax coronal spectrograms, and compared the deflections with those due to the sensitometric spots. (2) We obtained spectra through the same instrument used for the coronal lines, of light from the solar disk, attenuated by various known amounts and compared densities in these spectra with sensitometric spot densities on the same plates; thus we established an equivalence between effective spot brightness and disk brightness at various wavelengths. (3) We compiled a table from the results of steps (1) and (2) that showed, for various sky brightnesses, the line intensities in equivalent Angstroms corresponding to various intensities in the old Climax scale. (4) We constructed a table of factors for obtaining the true green line/red line ratio from the apparent ratio for each emulsion used. Finally (5) we compared Climax coronal line intensities in equivalent angstroms with those given by other stations. A more detailed description of these steps follows.

B. Details of the Procedure.

Step 1. We made approximately 750 microphotometer tracings of coronal line profiles using the High Altitude Observatory microphotometer. The intensities indicated by these profiles were expressed in terms of the uncalibrated but controlled intensity scale used for making the sensitometric spots. These intensities were grouped according to sky brightness, and for each range of sky brightness, a graph of the type shown in Figure 1 was plotted from each year's data analyzed. We were able to detect a clear-cut change in slope of the correlation lines on these graphs with increasing sky brightness. We were not, however, able to effect a significant reduction in the scatter of the points by introducing corrections for variation in spot density or gamma. Hence we concluded that sky brightness was the most significant extraneous parameter entering into the reading of line intensities by the

Climax comparison method. Our assumption that the use of the microphotometer for determining line intensities adequately compensated for variation in sky brightnesses was verified by a special experiment: R. T. Hansen, observer-in-charge at Climax obtained a series of spectra of the same coronal line. After photographing the spectra, he artificially increased the backgrounds various degrees by superimposing spectra of the sky far from the sun on the coronal spectra. Line intensities from the various spectra determined by visual comparison with the comparison lines showed a steady and serious decrease with increasing background, whereas those determined by the microphotometer were essentially independent of background.

Step 2. We attenuated light from the solar disk to intensities commensurate with coronal intensities by means of an opalized glass placed directly in front of the coronagraph objective. To illustrate the principle of the action of the opalized glass we first consider the glass to be an ideal diffuser, i.e. absorbs no light, but one that scatters any light incident upon it equally well forward or backward according to Lambert's Law. Without the opalized glass, the light striking any element of the surface of the coronagraph lens is contained in a solid angle $= A_\odot/R^2$, where $A_\odot$ is the area of the solar disk and where R is the distance from the sun to the earth. Let the mean flux density of the light in this cone be J ergs/sec/unit solid angle. If the opalized glass is inserted this flux is scattered over a sphere. Let the flux density of the scattered light normal to the scattering surface be J' ergs/sec/unit solid angle. Then, since the incident flux must equal the outgoing flux

$$2\int_0^{\pi/2} 2\pi J' \sin\phi \cos\phi \, d\phi = J A_\odot / R^2$$

and $J'/J = A_\odot/2\pi R^2$.

If r = the solar radius,

$$J'/J = \tfrac{1}{2}(r/R)^2 = 10.8 \times 10^{-6}.$$

If we introduce limb darkening data so as to express scattered flux density in terms of density of flux from the center of the solar disk, the attenuation factor J'/J depends on wavelength, and is 8.49×10^{-6} for $\lambda 5303$ and 8.88×10^{-6} for $\lambda 6374$.

We determined, by laboratory measurements, the extent of the departure of our particular piece of opalized glass from an ideal glass. For these measurements we used a collimated beam of light, produced by placing a cylindrically coiled automobile headlight filament at the focus of a collimating lens, with the long axis orientated along the lens axis. This light was

allowed to fall normally upon the surface of the opalized glass. The detector consisted of a lens that focused an image of the plane of opalized glass on a variable aperture, the aperture being directly in front of the photosensitive surface of a 1P41 photocell. A microammeter and a 22.5 volt dry cell in series with the photocell completed the apparatus. See Figure 2.

In this arrangement, we first confirmed by use of various apertures that the detector response was linear over the range of light levels used. Then we measured the photocurrent with the opalized glass in place and the detector placed so as to receive light scattered at various angles, and also with the opalized glass removed and the detector receiving light directly from the surface.

Let D_1 be the deflection of the detector when the opalized glass is in place; D_2 be the deflection when the opalized glass is removed, Ω be the solid angle subtended at a point on the plane of the opalized glass by the detector lens, I = collimated light incident on the opalized glass within the circle defining the image of the detector aperture when the detector is in line with the source; S = scattered light, per unit solid angle, from the same circle in the opalized glass.

Then:

$$\frac{S\Omega}{I} = \frac{D_1}{D_2} .$$

For an ideal opalized glass S is constant and:

$$2\int_0^{\pi/2} 2\pi S \sin\phi \cos\phi \, d\phi = I.$$

Our experiment showed that the forward scatter of our opalized glass was, within the limits of accuracy of our experiment, equal to that which we would expect from an ideal glass. A more detailed investigation, made by placing the detector at various angles with the incident beam, indicated a distribution of S with angle as shown in Figure 3. A numerical integration of the intensity over the entire sphere accounted for about 85% of the light. Thus it would appear that, for forward scattering, a small specularity almost exactly compensated for the absorption in the glass.

Having calibrated the opalized glass, we manufactured a step slit with widths of 2, 4, 8, 16 and 32 times that used in routine spectroscopy of the corona. We then photographed ten spectra of the solar disk, with the step slit in the spectrograph and the opalized glass over the objective lens of the coronagraph. The dust-cover limited the amount of sky illuminating the diffusing glass to a few degrees from the sun, thus making unnecessary a correction that would have been very difficult to compute had the glass been

exposed to a significant portion of the sky. The plates containing the disk spectra were spotted in the same sensitometer that is used in all routine coronal plates, and the spot densities were then compared with densities in the disk spectra. The comparison was carried out at wavelengths near 1up. λ5303, λ5694, λ6374 and Ha, but sufficiently removed from any major absorption lines that their wings, extensive in the cases of the broad slits, did not influence the results. From this comparison, we arrived at the set of lines shown in Figure 4. Since the sensitometric spots were made with green light, we would expect the line in Figure 4 for λ5303 to hold for all photographic emulsions. The slope of other lines would vary with the color sensitivity of the emulsion, however.

Step 3. In compiling the tables for converting Climax arbitrary into absolute intensities, we selected from the various graphs of the type shown in Figure 1, points from curves that seemed to be best established. These were arranged on a plot of spot-scale intensities vs. sky brightness, as shown in Figure 5, and curves were drawn through points of equal Climax arbitrary scale intensities. These curves were so drawn that not only would they be smooth, but that their spacing would be systematic. Thus the entire aggregate of several hundred microphotometer tracings went into the fixing of each equivalence between the Climax arbitrary scale and the spot scale. The tables were compiled by reading values of spot scale intensity from Figure 5 and translating them into equivalent Angstroms by means of Figure 4. A complete table is given in Appendix I.

Step 4 required the determination of the relative spectral sensitivity of the emulsions that have been used in the past at Climax. To do this we measured the apparent brightness of the sky at various wavelengths, in spot-scale units, for representative plates of different emulsions. Then, assuming that the color distribution in the sky had actually been the same for all spectra, we compared the apparent color distribution with that found by comparing sky to disk spectra. Our assumption of a sky of unchanging color was justified to some extent by an analysis of the background on certain coronal spectra that were photographed on the same plates as the disk spectra. Although the background brightness varied over a rather wide range on these plates, the ratios between intensities at various wavelengths remained very nearly constant. A table of factors for multiplying apparent intensity ratios for various emulsions used at Climax in the past in order to get true intensity ratios is given in Appendix II. We note that during the years 1945-1954 the red sensitivity of the plates has increased progressively, giving an apparent gradual decrease in green/red ratio.

For Step 5 we plotted Climax absolute intensities, obtained using the tables, vs. Pic du Midi and Wendelstein absolute intensities for the years

1947, 1949, 1951 and 1953. The results are shown in Appendix III. Each point represents the maximum intensity given in a solar limb quadrant on a given day, as determined by Climax and the other station. Wendelstein data were converted to absolute values by the formula given by Kraul (1954). We draw the following conclusions from this comparison: (1) Points are badly scattered. (2) At times of high solar activity, there appears to be a 1-1 correspondence between the range of intensities observed at Wendelstein and those observed at Climax, whereas the Pic du Midi intensities are approximately twice as great as for Climax. (3) At times of low solar activity, Wendelstein intensities range approximately twice those at Climax, and Pic du Midi intensities four times as great.

Some investigations that we have carried out recently at Climax offer a tentative explanation for these discrepancies. In our routine operation, the Climax coronagraph is adjusted so that the sun is focused on the occulting disk in $H\alpha$, whereas the occulting disk is focused on the spectrograph slit in green. The result is that features of the sun are most clearly focused on the spectrograph slit in a wavelength in the approximate orange part of the spectrum, while the circle of confusion for green is approximately 60,000 km. in diameter. Observations are made at fixed distances from the solar limb. Wendelstein makes observations with all apparatus in focus in green. Pic du Midi, when observing the green coronal line, also focuses the apparatus in green, but uses a radial slit. Thus Pic du Midi intensities can represent the maximum values at the height of brightest corona. We have found in one case recently that by changing the Climax focus to green throughout and bringing the slit as close to the image of the limb as possible we were able to increase the brightness of a coronal region in λ5303 from 12 millionths to 38 millionths of an equivalent angstrom. The brightness determination of another region, similarly studied, increased from 34 to 97 millionths. From the data that we took we were able to draw isophotal contour maps of the two regions, and found that the intensities on these maps, averaged over the known circle of confusion, agreed very closely with those found by routine observations. At times of high coronal activity the regions are more extensive, so our results have not been so sensitive to the sharpness of the focus, but at times of low activity the regions are both less extensive along the limb and lie closer to it.

A new spectrograph, soon to be installed at Climax, will give us, on a routine basis, in-focus observations for each line studied. Climax absolute intensities may then be expected to agree more closely with those of other stations at all times in the solar cycle. Our experience points out, however, the importance of all stations clearly specifying the height above the limb at which observations are made.

The authors wish to express their appreciation to Dr. Walter Orr Roberts for his advice and for his enthusiastic support of the project; to the Climax Observers for the many excellent special plates used in the investigation, especially to Mr. R. T. Hansen who initiated much of the work that got the standardization program under way; to Dr. Gerard Wlerick, for checking the mathematics involved in the basic assumptions of the program and computing the performance characteristics of the Climax coronagraph as it is now operated; and finally to a number of our colleagues who have, from time to time, discussed the program and given us valuable suggestions; Dr. R. G. Athay of the High Altitude Observatory; Dr. Harold Zirin of Harvard College Observatory; Dr. J. W. Evans and Dr. C. S. Yü of the Upper Air Research Observatory.

BIBLIOGRAPHY

Behr (1951) Zs. f. Ap. 28, 296.

Bell and Glazer (1953) Solar Department of Harvard College Observatory. Scientific Report No. 12.

Bruzek (1955) Zs. f. Ap. 35, 213.

Transactions of I. A. U. (1952) 8, 151.

Kraul (1954) Zs. f. Ap. 33, 174.

Waldmeier (1951) Die Sonnenkorona I (Verlag Birkhäuser Basel) p. 24.

Figure 1.

Green Line - Thresholds 11, 12, 13 - Year 1947.

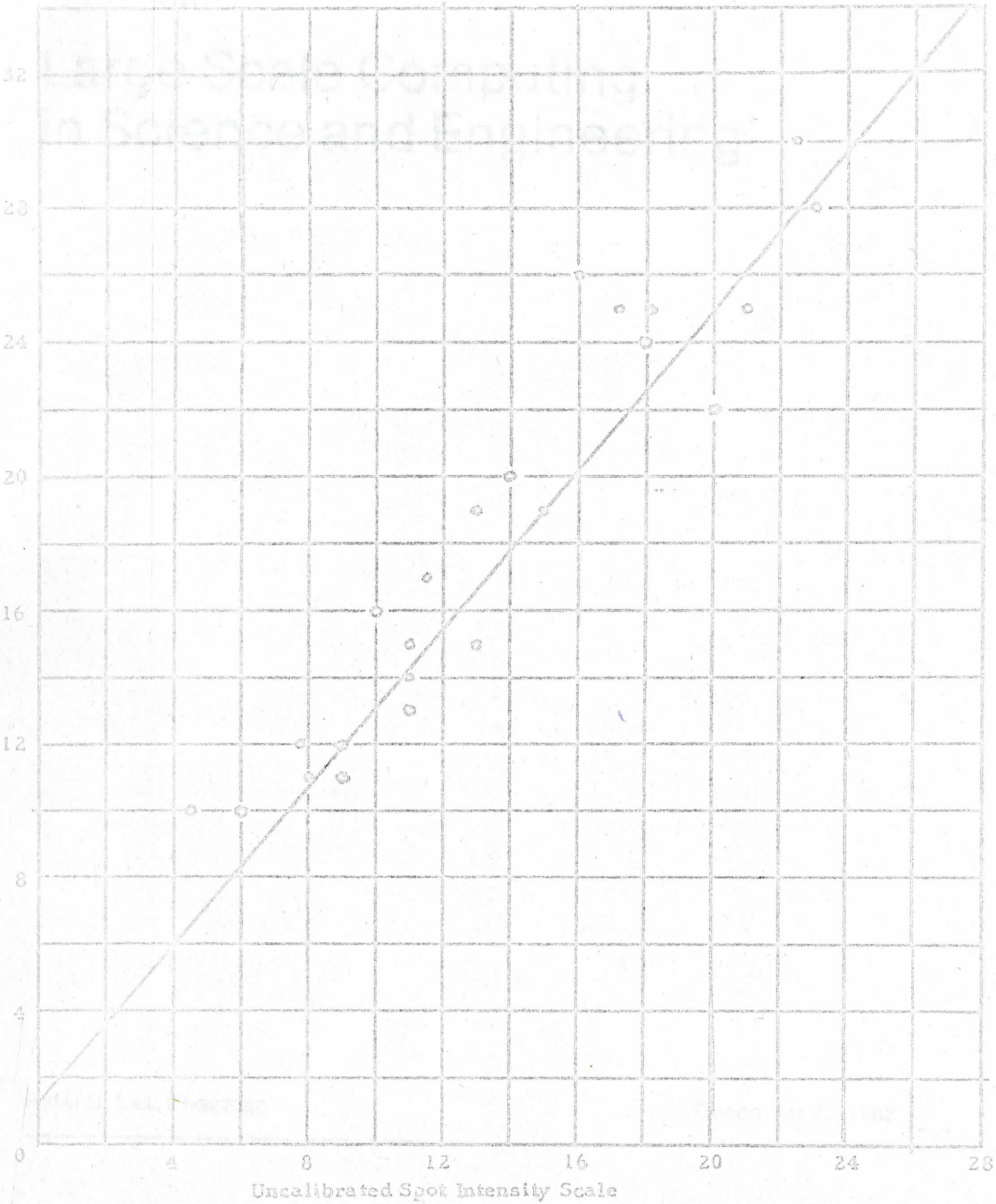

Figure 2

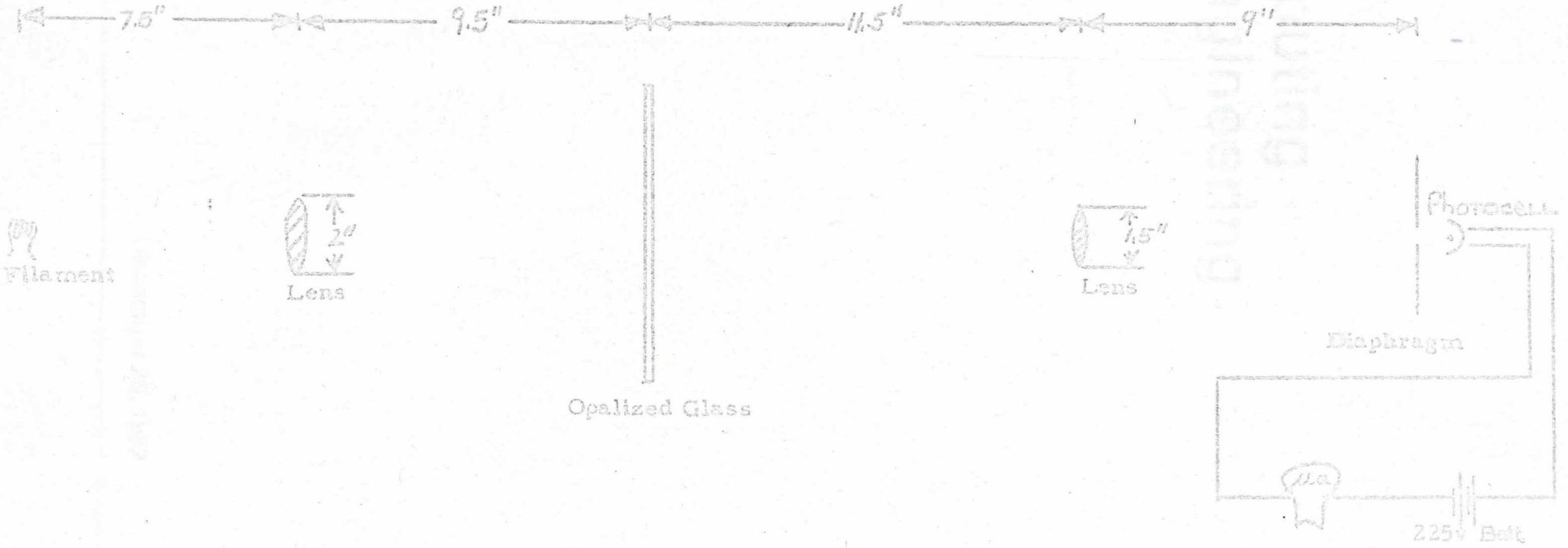
7.5"
9.5"
11.5"
9"
Filament
2"
Lens
Opalized Glass
1.5"
Lens
Photocell
Diaphragm
225 V Batt.

Figure 3

Actual Scattered Light

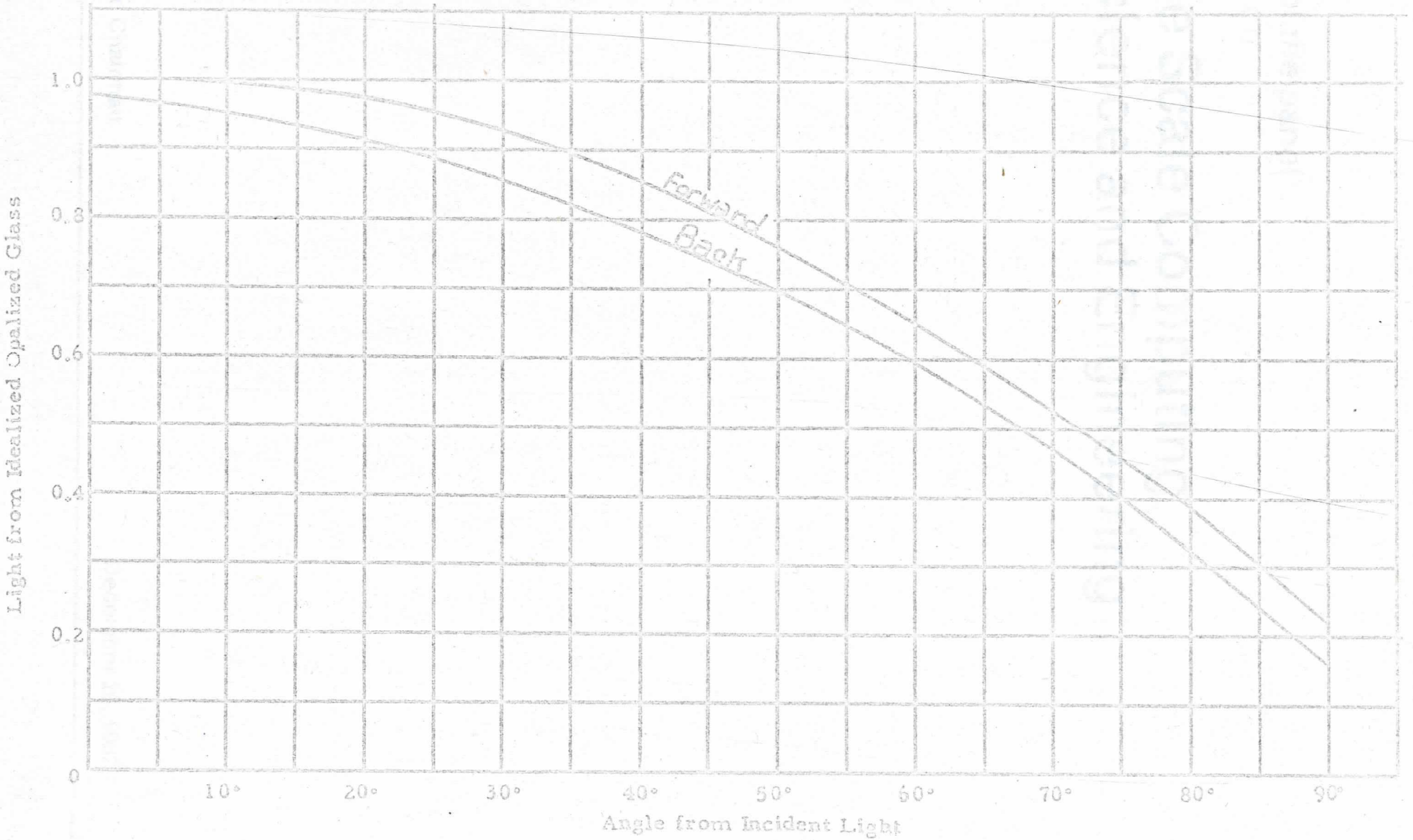

Figure 4.

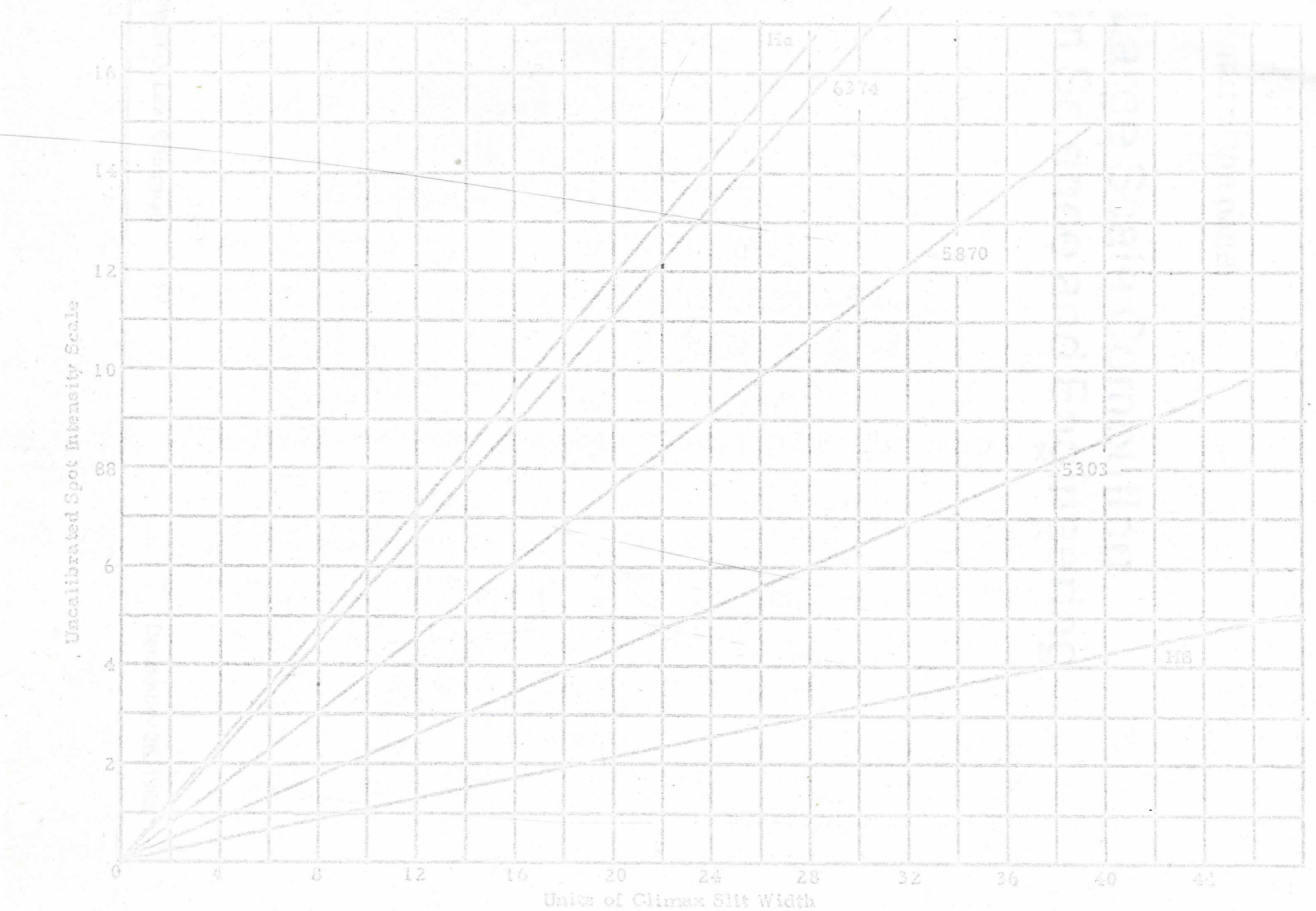
Ha
6074
5870
5303
HB
16
14
12
10
8
6
4
2
0
4
8
12
16
20
24
28
32
36
40
44
Uncalibrated Spot Intensity Scale
Units of Climax Slit Width

Figure 5 = 6374 Å

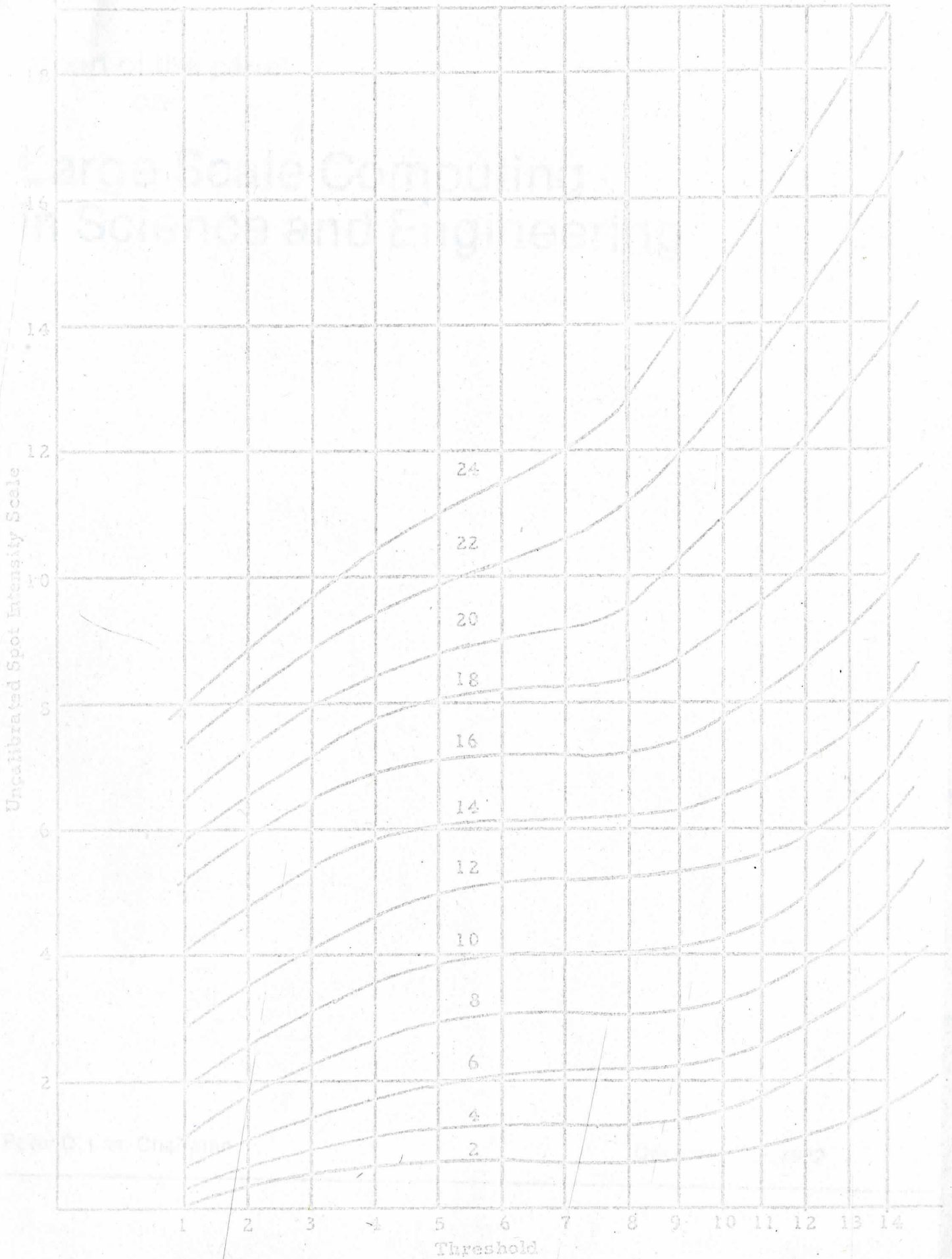

Appendix I

Visual Reading	Threshold (λ 5303 A)												
	1	2	3	4	5	6	7	8	9	10	11	12	13
1	0.2	0.4	0.4	0.4	0.7	0.7	0.7	1	1	1.5	1.5	2	2
2	0.4	0.7	0.7	1	1.5	1.5	1.5	2	2	3	3	3	4
3	0.7	1	1	2	2	2	2	3	3	4	5	5	6
4	1	1.5	2	3	3	3	3	4	4	5	6	7	8
5	1.5	2	3	3	4	4	4	5	5	6	7	8	9
6	2	3	3	4	5	5	5	6	7	7	9	9	10
7	2	3	4	5	5	6	6	7	8	9	11	11	12
8	3	4	5	6	6	7	8	8	9	10	13	13	14
9	4	5	7	8	9	9	9	10	12	13	15	16	18
10	5	7	9	11	12	12	12	13	14	16	18	20	21
11	7	9	11	13	14	14	15	15	17	19	21	23	25
12	8	11	14	15	17	17	18	18	20	23	25	26	29
13	9	13	16	18	19	19	20	21	23	25	27	29	32
14	11	15	18	20	21	21	22	23	25	28	30	32	35
15	13	18	21	23	24	25	25	26	29	31	33	35	38
16	15	20	24	26	27	27	28	29	31	34	36	39	41
17	18	22	26	28	29	30	30	32	34	37	39	41	44
18	20	25	29	31	32	32	33	35	36	40	42	45	48
19	22	27	31	33	34	35	35	37	40	43	45	48	50
20	25	30	33	35	37	37	38	40	43	46	48	50	53
21	28	32	36	38	39	40	41	44	47	49	52	55	58
22	31	35	39	41	42	44	45	47	50	53	57	59	64
23	34	38	41	43	45	47	48	51	54	57	60	64	67
24	36	40	43	45	47	49	52	54	57	61	65	67	71
25	38	42	45	47	50	53	56	59	62	66	70		
26	40	44	47	50	52	57	60	64	67	72			
27	42	46	49	52	55	59	63	66					
28	44	47	51	54	58	62	65	69					
29	45	49	53	57	60	65	68						
30	46	51	55	59	63	67	71						
31	48	53	57	61	66	70							
32	49	55	59	64	68	75							

Appendix I (Cont.)

Exposure time (sec)	Threshold (λ; 6374 A)													
	1	2	3	4	5	6	7	8	9	10	11	12	13	14
1	0.1	0.4	0.4	0.6	0.6	0.6	0.8	0.8	0.8	1	1	1	1.5	1.5
2	0.2	0.6	0.8	1	1	1	1	1	1.5	1.5	2	2	3	3
3	0.4	0.8	1	1.5	1.5	1.5	2	2	2	2	3	3	4	4
4	0.6	1	1.5	2	2	2	2	3	3	3	3	4	4	6
5	1	1.5	2	2	3	3	3	3	3	4	4	5	5	6
6	1	2	2	3	3	4	4	4	4	4	5	5	6	7
7	1.5	2	3	4	4	4	4	5	5	5	6	6	7	8
8	2	3	4	5	5	5	5	6	6	6	7	7	8	9
9	3	4	5	6	6	6	6	7	7	7	8	8	9	10
10	4	5	6	7	7	7	7	7	8	8	9	9	10	11
11	4	6	7	8	8	8	8	8	8	9	9	10	11	12
12	5	7	8	9	9	9	9	9	9	10	10	11	12	13
13	6	8	9	10	10	10	10	10	10	11	11	12	13	14
14	7	9	10	11	11	11	11	11	12	12	12	13	14	15
15	8	10	11	12	12	12	12	12	13	13	14	15	16	16
16	9	11	12	12	13	13	13	13	14	14	15	16	17	18
17	10	11	12	13	14	14	14	14	15	16	16	17	19	19
18	11	12	13	14	15	15	15	15	16	17	18	19	20	22
19	11	13	14	15	16	16	16	16	17	18	19	22	22	23
20	12	13	15	15	16	16	16	17	19	20	20	23	24	26
21	12	14	15	16	17	18	18	19	20	22	23	25	26	28
22	13	15	16	17	18	19	19	20	22	24	25	27	28	30
23	14	15	17	18	19	20	20	22	24	26	27	29	31	
24	15	16	18	19	20	21	21	24	26	28	29	32	34	

Appendix II

Date	Emulsion	K(red line)	K(yellow line)
1945	266696	0.765	0.763
1945	300854	0.695	0.774
1946	316605	0.630	0.804
1947	No record	0.654	0.756
1948	No record	0.617	0.732
1949	No record	0.645	0.707
1950	442408	0.442	0.626
1950	456680	0.382	0.636
1951	459580	0.346	0.561
1951	462435	0.638	0.853
1951	476691	0.420	0.660
1952	485149	0.397	0.674
1953	VEC 2L2	0.479	0.682
1954	494600	0.402	0.608
1954	496582	0.383	0.565

Appendix III

Calibration of Climax vs. Pic du Midi - 1947

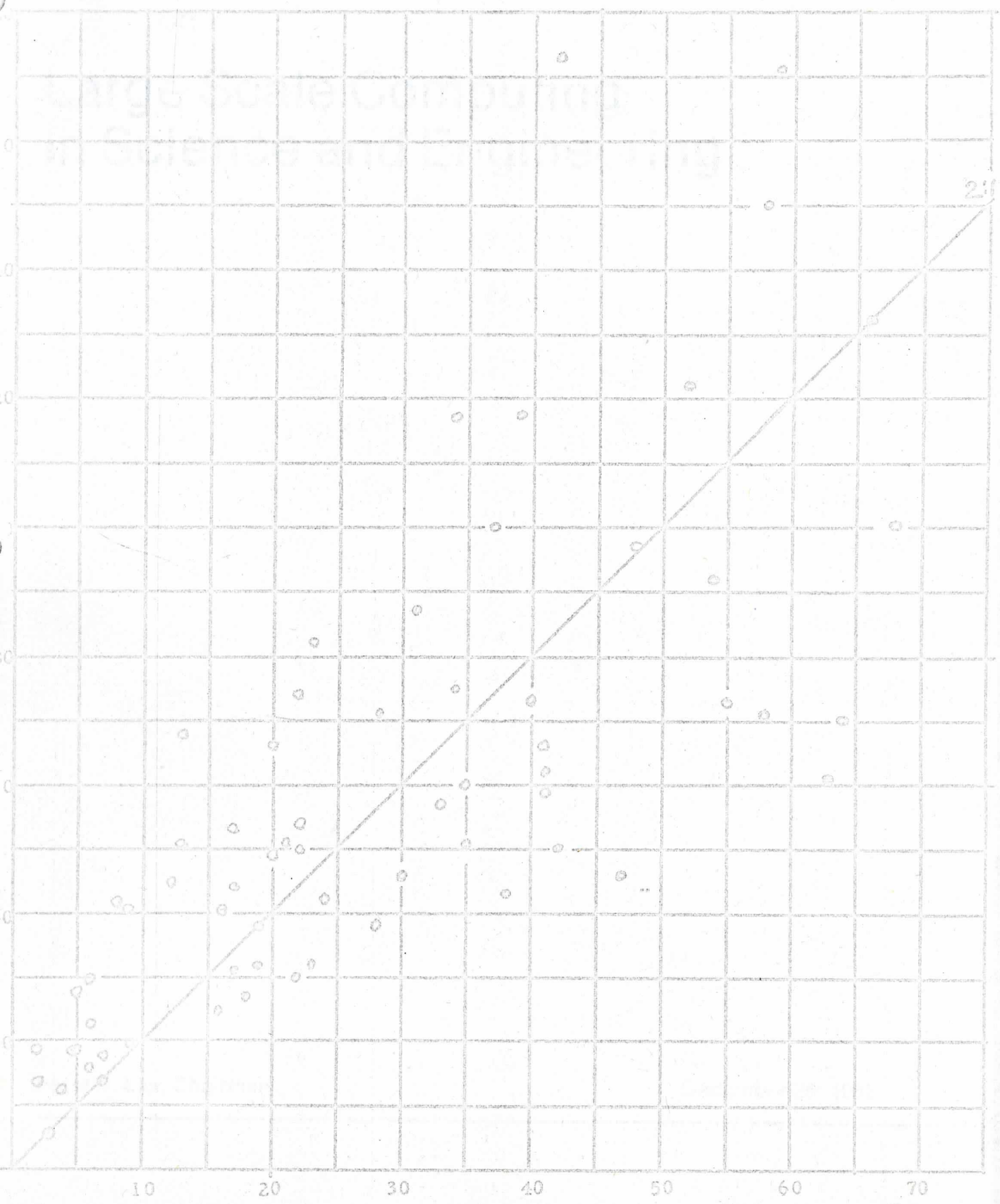

Appendix III (cont.)

Calibration of Climax vs. Wendelstein - 1947

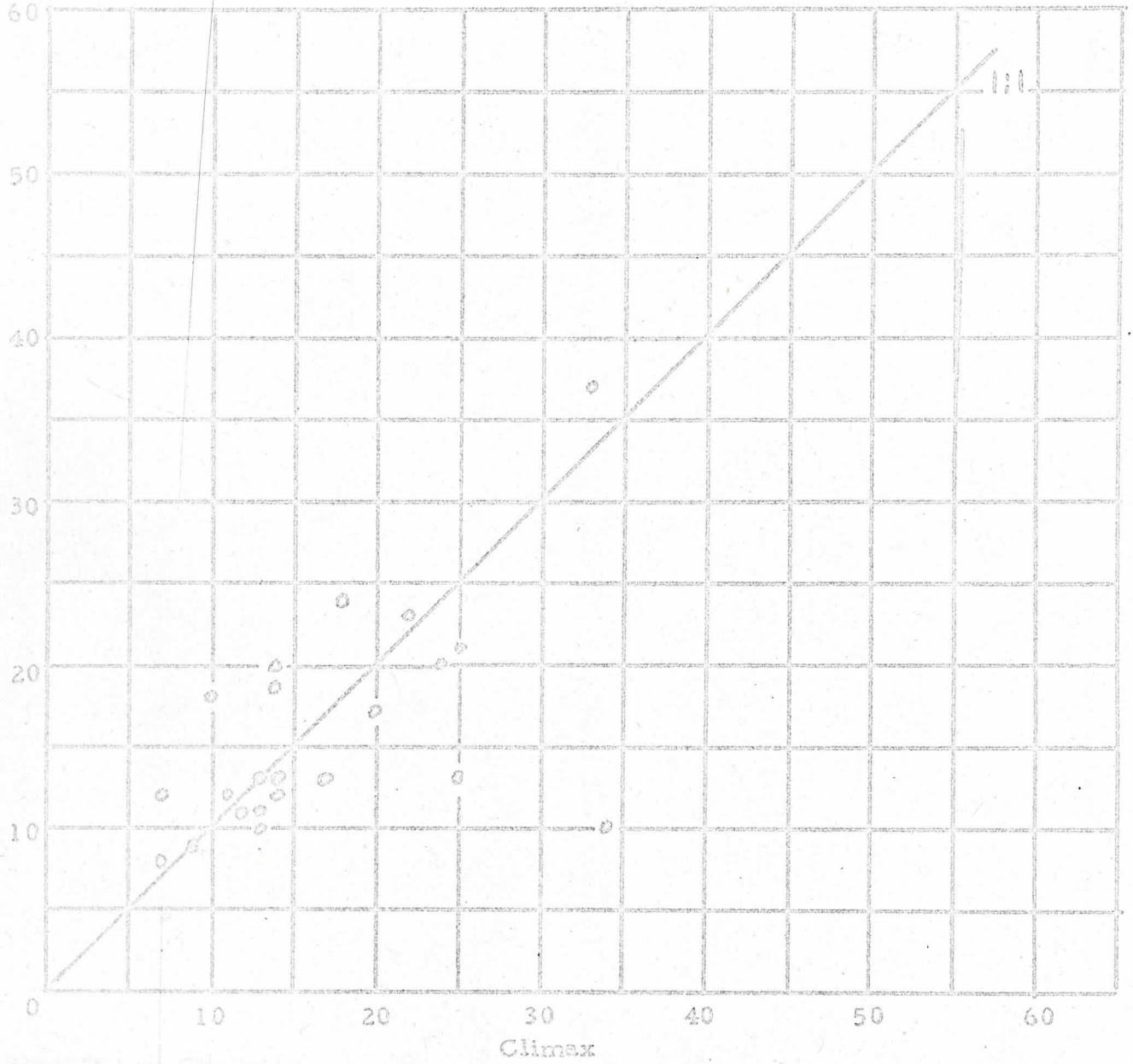

Appendix III (cont.)

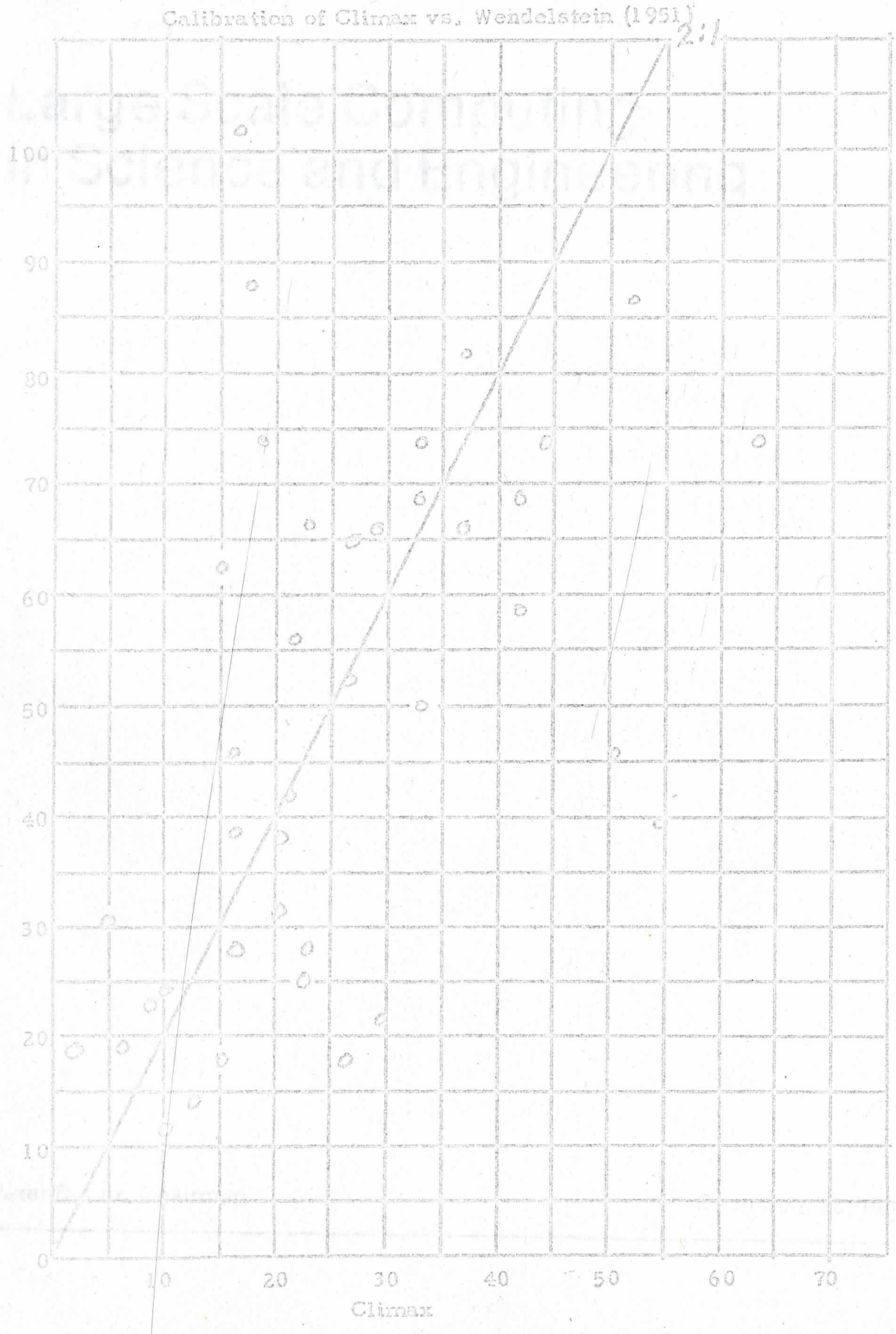

Appendix III (cont).

Calibration of Climax vs. Pic du Midi - 1953